Targeted Intervention of eIF4A1 Promotes EMT and Metastasis of Pancreatic Cancer Cells through c-MYC/miR-9 Signaling

Yuchong Zhao
Tongji University
Yun Wang
Tongji Hospital of Tongji Medical College of Huazhong University of Science and Technology
Wei Chen
Tongji Hospital of Tongji Medical College of Huazhong University of Science and Technology
Shuya Bai
Tongji Hospital of Tongji Medical College of Huazhong University of Science and Technology
Wang Peng
Tongji Hospital of Tongji Medical College of Huazhong University of Science and Technology
Mengli Zheng
Tongji Hospital of Tongji Medical College of Huazhong University of Science and Technology
Yang Yilei
Tongji Hospital of Tongji Medical College of Huazhong University of Science and Technology
Bin Cheng (b.cheng@tjh.tjmu.edu.cn)
Tongji Hospital of Tongji Medical College of Huazhong University of Science and Technology
https://orcid.org/0000-0003-1568-8760
Zhou Luan
Tongji Hospital of Tongji Medical College of Huazhong University of Science and Technology

Primary research

Keywords: eukaryotic translation initiation factor 4A1, c-MYC, epithelial-mesenchymal transition, rocaglamide, mycro3

Posted Date: September 21st, 2021

DOI: https://doi.org/10.21203/rs.3.rs-907935/v1

Abstract

Background: Due to the lack of effective interference options, early metastasis remains a major cause of pancreatic ductal adenocarcinoma (PDAC) recurrence and mortality. However, the molecular mechanism of early metastasis is largely unknown. We characterize the function of eukaryotic translation initiation factors (eIFs) in Pancreatic cancer cell epithelial mesenchymal-transition (EMT) and metastasis, to investigate whether it is effective to inhibit EMT and metastasis by joint interference of eIFs and downstream c-MYC.

Methods: We used the data of The Cancer Genome Atlas (TCGA) and Genome Tissue Expression (GTEx) to analyze the expression level of eIF4A1 in PDAC tissues, and further validated in a microarray containing 53 PDAC samples. Expression regulation and pharmacological inhibition of eIF4A1/c-MYC was performed to determine their role in migration, invasion, and metastasis in pancreatic cancer cells in vitro and in vivo.

Results: Elevated expression of eIF4A1 was positively correlated with lymph node infiltration, tumor size, and indicated a poor prognosis. eIF4A1 decreased E-cadherin expression through c-MYC/miR-9 axis. Ablation of eIF4A1 and c-MYC decreased the EMT and metastasis capabilities of pancreatic cancer cells. Upregulation of eIF4A1 could attenuate the inhibition of EMT and metastasis induced by c-MYC downregulation. Single-use of eIF4A1 inhibitor Rocaglamide (RocA) or c-MYC inhibitor Mycro3 and joint intervention all significantly the EMT level of pancreatic cancer cells *in vitro*. However, the efficiency and safety of RocA single-use were not inferior to joint use *in vivo*.

Conclusion: The results demonstrated that overexpression of eIF4A1 downregulated E-cadherin through c-MYC/miR-9 axis, which promoted EMT and metastasis of pancreatic cancer cells. Despite the potential loop between eIF4A1 and c-MYC existing, RocA single strategy was a promising therapy for the inhibition of eIF4A1 induced PDAC metastasis.

Introduction

Pancreatic ductal adenocarcinoma (PDAC) is one of the most lethal solid malignancies universally. Despite a relatively low incidence, it remains the fourth leading cause of cancer-related deaths in developed countries (1, 2). There were no significant changes in the mortality to incidence ratio during the past decades. The five-year survival rate remains about 3%-15% (3). At the early stage of carcinogenesis, pancreatic cancer cells could metastasize to distant organs through epithelial-mesenchymal transition (EMT) (4). An overwhelming majority of PDAC preliminary diagnosis patients have lost the chance of surgical eradication due to early metastasis, which is also the key reason for post-operation recurrence. KRAS was the most common oncogenic mutations associated with PDAC (5). So far, all the attempts targeted common PDAC KRAS variants (e.g., G12D, G12V, G12R) and multiple KRAS downstream kinases (e.g., RAF, MEK, ERK, PI3K) failed in □/□ clinical trials (6–9). Thus, novel therapeutics other than KRAS-associated kinases targeted inhibitors are urgently needed for PDAC patients.

Uncontrolled protein production is a symbolic characteristic of cancer cells, and it is also necessary for EMT and metastasis (10). Therefore, the intervention of the hyperactive protein production becomes a possible therapeutic for PDAC. Translation initiation regulated by eukaryotic translation initiation factors (eIFs) is the most important rate-limiting procedure in translation (11, 12). Dysregulation of eIFs is a hallmark of various types of cancers including PDAC, among which eIF4F heterotrimeric complex is the main factor to facilitate mRNA translation. Meanwhile, the activity of eIF4F is largely regulated by RAS signaling, which further indicated eIF could play an important role in PDAC(13, 14). The eIF4F complex is composed of the scaffold protein eIF4G, cap-binding protein eIF4E, and ATP-dependent DEAD-box RNA helicase eIF4A. Previous studies typically chose eIF4E as the target to inhibit the EMT and metastasis of cancer cells, because eIF4E was generally overexpressed in multiple cancers. However, recent studies demonstrated that there existed eIF-independent yet eIF4A-dependent binding sites of eIF-downstream oncogenic mRNA including c-MYC, which was the possible reason why the trials targeted eIF4F did not work (15, 16). eIF4A is the only regulatory enzyme-catalytic factor in eIFs, which facilitates unbinding the complex long-sequence helix (CLSH) in mRNA 5’-untranslated region (5’-UTR). And the CLSH is a typical signature of various eIF-downstream mRNA including c-MYC (17). The overexpression of c-MYC is a carcinogenesis driver for multiple cancers and c-MYC was the most activated Oncogenes (18, 19). c-MYC was a crucial regulator for EMT and metastasis through promoting miR-9 expression (20, 21). However, due to the structure of c-MYC, there were few c-MYC targeted inhibitors by now (22, 23). Considering eIF4A being dispensable for c-MYC translation, we hypothesized that intervention of eIF4A could be an effective way for c-MYC inhibition.

Traditional Chinese medicinal herbs gained our attention as a novel source of anticancer remedies during the past few years. Rocagalamide (RocA) was a cyclopenta-b-benzofuran-type compound derived from traditional Chinese remedies genus *Aglaia* (family *Meliaceae*). Iwasake *et al.* carried out a survey in 2016 that RocA could attach eIF4A firmly at the 5’-UTR sequence and thus suppress the hyperactive protein production than the intervention of eIF4E (24). Subsequently, RocA was used in various hematologic malignancies (e.g., myeloma, T-cell lymphoma) and exerted a prominent anti-tumor efficacy without observed side effects in mouse model (25). The trials of RocA in solid malignancies were rare, and one of those was our previous study which demonstrated that RocA obviously repressed the EMT and metastasis of pancreatic cancer cells in the mouse model (26). Nevertheless, how eIF4A was involved in the EMT and metastasis of PDAC was still largely unknown. And taken the complex loop relation between eIF4A and c-MYC, whether eIF4A and c-MYC dual inhibition were superior to the single-therapeutic intervention deserved to be investigated. There are 3 identified isoforms eIF4A in human. eIF4A1 is the major type to participate in the assembly of eIF4F in cancer cells and eIF4A2, which is mainly expressed in low-level proliferating cells, is correlated with a good prognosis in multiple cancers (12, 17). Therefore, we selected eIF4A1 as the target in follow-up studies.

Here, we reported that overexpression of eIF4A1 downregulated the expression of E-cadherin through c-MYC/miR-9 signaling axis, which promoted EMT and metastasis.

Materials And Methods

Cell culture and reagents

Immortalized pancreatic ductal epithelial cell line (HPDE) and pancreatic cancer cell line (Canpan-2) were obtained from the Cell Bank of the Chinese Academy of Sciences (Shanghai, China), and pancreatic cancer cell lines (AsPC-1, BxPC-3, Panc-1) were purchased from the American Type Culture Collection (VA, USA). The cells were cultured in RPMI-1640 medium (GIBCO, NY, USA) supplemented with 10% fetal bovine serum (FBS, GIBCO) and 1% penicillin/streptomycin (Invitrogen) at 37°C in a 5% CO_2 incubator. The eIF4A inhibitor RocA and c-MYC inhibitor mycro3 were purchase from MedChemExpress (MCE, USA).

Patients' follow-up and specimens

This study was approved by the Ethics Committee of Tongji Hospital of Tongji Medical College, Huazhong University of Science and Technology (TJ-IRB20210927). All patients have been completely informed of the possible use of the clinical information/specimens and we obtained full consent for the study. The cohort included 53 patients with PDAC who underwent surgical resection from 2009 to 2013 at the Department of Pancreatic and Hepatobiliary Surgery, Tongji Hospital of Tongji Medical College, Huazhong University of Science and Technology (Wuhan, China). All the PDAC specimens were verified by pathologists and met the criteria of the American Pancreatic Association. All the patients did not accept pre-operative neoadjuvant therapy. The patients were evaluated every 3 months during the first 3 years and every 6 months thereafter performed by physicians who were blinded to this study. Follow-up data were summarized at the end of December 2020. To evaluate the prognostic role of eIF4A1, tissue microarrays of 53 PDAC samples were collected for immunohistochemistry (IHC).

Immunohistochemistry (IHC)

IHC staining with the eIF4A1 antibody (Abcam ab31217) was performed to detect the protein expression level. Assessments of microarray IHC staining were performed by ImageJ (http://imagej.nih.gov/ij) IHC profiler (http://sourceforge.net/projects/ ihcprofiler). The intensity of staining was scored on a scare as negative (0 points), weak-positive (1 point), positive (2 points), and strong-positive (4 points). The protein expression level was calculated by multiplying the staining intensity and corresponding positive staining extent n (n%: percentage of positive areas to the whole areas). Then we divided the patients into two groups (grade < 50, low expression; grade > 50, high expression) and performed subsequent survival analysis. The results of IHC staining were reassessed by two independent pathologists who were blinded to this study.

Immunofluorescence

Paraformaldehyde fixed samples were washed 3 times with cold PBS for 3min each time and then incubated in 10% donkey serum in PBS for 20min. Subsequently, then the samples were incubated with the eIF4A1 antibody (Abcam ab31217) in PBS at 4°C overnight. After washing, fluorochrome-conjugated

secondary antibodies (1:400, Alexa Fluor®488 donkey anti-rabbit IgG) were used, and then the samples were incubated with DAPI. Fluorescence was visualized under an Olympus microscope.

Lentivirus

Lentivirus vector encoding shRNAs was generated using pLVX-Puro (Addgene) obtained from DesignGene Biotechnology (Shanghai, China). The vectors were designated as Lv-eIF4A1 (eIF4A1-1: 5'-CACACTGGACTAGTGGATCCCGCCACCATGTCTGCGAGCCAGGATTCCC-3'; 5'-AGTCACTTAAGCTTGGTACGATGAGGTCAGCAACATTGAGG-3'), Lv-sh-c-MYC (c-MYC-1: 5'-GCTTCACCAACAGGAACTATG-3'; c-MYC-2: 5'-GCTTGTACCTGCAGGATCTGA-3'; c-MYC-3: 5'-GGAAACGACGAGAACAGTTGA-5') and non-target Lv-sh-control (empty vector). The lentivirus plasmid and packaging plasmids were transfected into pancreatic cancer cells with transfection reagent (Lipofectamine®3000, Thermo Fisher Scientific) and OPTI-MEM media (Invitrogen, MA, USA). Lentiviral infection of target cells was performed in cell culture medium with 5μg/ml polybrene (Sigma H9268) selected with 2.5μg/ml puromycin for follow-up experiments.

Quantitative Real-time PCR (RT-qPCR)

The cDNA was created according to the manufacture's protocol (PrimeScript^{TM}RT reagent Kit Perfect Real Time, Takara, RR037A). Quantitative PCR was performed on StepOne Real-Time System (Thermo Fisher Scientific) using TB Green® Premix EX Taq™ (Takara, RR820a) as the protocol. Melting curve analysis was performed and the amplification plots were evaluated by SDS 1.9.1 software (Applied Biosystems, MA, USA). The $2^{-\Delta\Delta Ct}$ method was used to determine relative fold changes in target gene expressions from replicate samples. The bulge-loop primer of miR-9 was provided by RioBIO (Guangzhou, China).

Western blot

Western blot analysis was performed as described previously (27). The primary antibodies include eIF4A1 (Abcam ab31217), c-MYC (Abcam ab32072), snail (Abcam ab216347), E-cadherin (Abcam ab40772), and Anti-β-actin (Abcam, ab8226). Immune complexes were visualized using the Beyo ECL Plus. The expression level was determined by ImageJ.

Transient transfection

The cells were transinfected with nonsense siRNA or siRNA targeting eIF4A1 (siRNA1: 5'-GAGTAACTGGAATGAGATT-3'; siRNA-2: 5'-TCCAGCAGCGAGCCATTC-3'; siRNA-3: 5'-CGTGTGTTTGATATGCTTA-3') and c-MYC (siRNA-1: GAGGAGACATGGTGAACCA; siRNA-2: GGGTCAAGTTGGACAGTGT; siRNA-3: CGACGAGACCTTCATCAAA) Lipofectamine®3000 (Thermo Fisher Scientific) and OPTI-MEM media (Invitrogen, MA, USA) according to the manufacturer's protocol. eIF4A1-siRNA-1 and c-MYC-siRNA-3 were the most effective siRNA and were used for further analysis. And cells were transfected with empty vector CV567, pcDNA3.1-eIF4A1 (P1: 5'-CACACTGGACTAGTGGATCCCGCCACCATGTCTGCGAGCCAGGATTCCC-3';) plasmids and pcDNA3.2-c-MYC plasmids (P1: 5'-CACACTGGACTAGTGGATCCCGCCACCATGGATTTTTTTCGGGTAGTGG-3';) using

transfection reagent Lipofectamine®3000 (Thermo Fisher Scientific) and OPTI-MEM media (Invitrogen, MA, USA) according to the manufacturer's protocol.

In vitro **migration and invasion assay**

Cell migration was analyzed using Transwell chambers (8-μm pore size; Millipore, Billerica, MA, USA), and cell invasion was analyzed using these Transwell chambers

with a Matrigel (BD Biosciences, San Jose, CA, USA) matrix. Cells were plated with FBS-free culture medium in the upper chamber and 10% FBS culture medium as a

chemoattractant. After 28h (Migration) or 32h (Invasion) of incubation, the low surface of the plates containing cells was washed with PBS, fixed in 4% methanol, stained with a 0.4% crystal violet solution. Photographs of three randomly selected fields of the fixed cells were captured and cells were counted. The experiments were repeated independently three times.

Metastatic model construction

This experiment with mice was approved by the Ethics Committee of Tongji Hospital of Tongji Medical College, Huazhong University of Science and Technology (TJH-202010007). Four-week-old female severe combined immune deficiency (SCID) mice (Charles River Co., Beijing) were maintained in specific pathogen-free (SPF) environments. Intravenous injection via caudal vein was used to establish the metastatic model *in vivo*. 200×10^6/200μl AsPC-1 cells were injected in each animal. Small animal imaging (Spectral Imaging LagoX) was performed every 3 days after cell injection and the mice were randomly divided into different groups for the following studies (n = 5/ group). The mice were sacrificed when the weight loss was greater than 20%. RocA (MCE, USA) was administrated by intraperitoneal injection (5mg/kg/d, 3mg RocA dissolved in 30μl DMSO, 600μl PEG300 and 75μl Tween-80 successively, then made the solution up to 1.5ml with normal saline) every day originally, then adjusted to 2.5mg/kg/d once on an alternate day. Mycro3 was administrated by intragastric (100mg/kg/d, 25mg mycro3 dissolved in 2.5ml 0.5% methylcellulose solution affiliated by ultrasound). The control group mice were treated by intragastric 200μl methylcellulose solution every day and 100 methylcellulose solution intraperitoneal cosolvent injection once on an alternate day.

Subcutaneous xenografts in nude mice

Four-week nude mice were obtained from HFK Bioscience Ltd (Beijing, China) and maintained in SPF conditions. AsPC-1 cells (5.0 × 106) suspended in a 100μl mixture of equal volumes of medium and matrix- gel were implanted subcutaneously into the right flank of 6-week-old female nude mice. When the tumors had reached a volume of about 60–90 mm3, the mice were then randomly divided into two groups. The treatment group received an intraperitoneal injection of RocA (previously adjusted dose), whereas the control group received cosolvent injection alone (n = 4). These treatments were carried out once daily for 28 days. Tumor volumes and the body weight of animals were measured twice a week. Tumor volumes (mm3) were calculated with the following formula: V = LS2/2 (where L is the longest

diameter and S is the shortest diameter). At the end of experiment, the mice were sacrificed and the tumors were harvested for western blot.

Statistical analysis

Data are representative of at least three independent experiments or multiple independent mice as indicated. The characteristics of patients were summarized as mean ± standard deviation (SD) for normally distributed continuous variables, median with interquartile range for continuous variables with skewed distribution, and frequency (percentage) for categorical variables. All the analyses were performed using R (http://www.R-project. org, version 3.5.2) with a two-sided significance threshold of $P < 0.05$.

Results

eIF4A1 was highly expressed in pancreatic ductal adenocarcinoma and predicted a poor prognosis

Firstly, we analyzed the expression of eIF4A1 in pan-cancer using data from Gene Expression Profiling Interactive Analysis (GEPIA, http://gepia.cancer-pku.cn/). eIF4A1 was highly expressed in multiple cancer types, including pancreatic adenocarcinoma, thymoma, glioblastoma multiforme, diffuse large B cell lymphoma, and testicular germ cell tumors (Fig. 1a). To evaluate the whole eIF family expression in pancreatic adenocarcinoma, we analyze the RNA-seq data from TCGA and GTEx. Two samples were deleted after data quality control, and finally, 179 cases of pancreatic tumor tissues and 169 cases of normal pancreatic tissues were obtained. We ranked differential expression of all the eIF (Fig. 1b) and the result showed that the expression level of eIF4A1 in pancreatic tumor tissues was significantly higher than in normal tissues (Fig. 1c).

Subsequently, we analyze the prognostic role of eIF4A1 in PDAC patients. eIF4A1 was mainly localized in the cytosol (Fig. 1d), which was consistent with the function of assisting translation initiation. We detected the eIF4A1 expression in a tissue microarray using immunohistochemistry from 53 PDAC patients confirmed by surgeries and pathologists from 2009 (Fig. 1e). The results indicated that patients with high eIF4A1 expression suggest a poor prognosis, the median OS of high eIF4A1 expression patients was significantly shortened compared with patients with low eIF4A1 (6.0 months VS 9.0 months, HR = 2.10, 95% CI: 1.44–5.24, P = 0.0061) (Fig. 1f). Furtherly, we examined the correlations between eIF4A1 expression and multiple clinical features (Table 1, * $P < 0.05$; χ^2 test or Fisher's exact test). Importantly, we found that a high level of eIF4A1 expression was significantly correlated with tumor size and lymph node metastasis. In summary, these results showed that eIF4A1 was highly expressed in pancreatic adenocarcinoma tissues, and high expression of eIF4A1 suggested a poor prognosis. The expression of eIF4A1 was positively correlated with lymph node metastasis which is a major way for cancer cell metastasis.

Table 1
Correlation between eIF4A1 expression and clinical characteristics of PDAC patients

Clinical Characteristics	High - eIF4A1	Low - eIF4A1	*P*-value
Age, mean ± SD, years	66.04 ± 9.69	64.10 ± 10.07	0.482
Male, n (%)	13 (56.53%)	21 (70.00%)	0.311
Overall survival, median, months	6.0 (4.0, 9.0)	9.0 (8.0, 15.5)	0.006*
Differentiation status			0.523
Well differentiated	11 (20.75%)	17 (32.08%)	
Moderately to poorly differentiated	12 (22.64%)	13 (24.53%)	
Tumor size, mean ± SD, cm	4.57 ± 1.40	3.75 ± 1.28	0.032*
Recurrences, n (%)	17 (73.91%)	20 (66.67%)	0.569
Location			0.267
Head, n (%)	15 (28.30%)	18 (33.96%)	
Body/tail, n (%)	7 (13.21%)	20 (37.74%)	
Diffusion involvement, n(%)	1 (1.89%)	2 (3.77%)	
TNM stage#			0.077
I – II stage, n (%)	14	24	
III – IV stage, n (%)	9	5	
Lymph node metastasis, n (%)	14 (63.64%)	10 (35.71%)	0.0498*
Vascular Infiltration, n (%)	10 (43.48%)	3 (10.00%)	0.272
# NCCN Version 3.2019 Pancreatic Adenocarcinoma			
* $P < 0.05$, significant difference			

eIF4A1 targeted c-MYC to regulate the metastasis in pancreatic cancer cells

To elucidate the mechanism underlying eIF4A1 regulating the biological behavior of tumor cells, we searched the GEO database for all the translational profiling by ribosome profiling that included pancreatic cancer cells, and ultimately, datasets GSE120159 was selected for further analysis. The data included 3 Panc-1 cell samples treated by rocaglate CR31B, a small-molecule inhibitor of the eIF4A helicase, and 3 Panc-1 cell samples treated by DMSO. A differential expression analysis using R package DEseq2 identified 179 differentially expressed proteins (DEP) between the CR31B-treated group and the

DMSO-treated group, with a *p.* adjusted (FDR) value < 0.05 and |log_2FC (fold change) |> 1 as the cut-offs. Among these proteins, 128 were downregulated and 51 were upregulated. The heatmap displayed the top overexpressed and suppressed molecules (Fig. 2a). The expression of c-MYC was significantly downregulated (log_2FC = -1.05, FDR = 0.00192) in the CR31B-treated group compared with the control group, ranked the top 0.6% in all the regulated gene lists.

To furtherly screen the key target of eIF4A to promote metastasis, we repressed the eIF4A1 expression (eIF4A1 siRNA) and analyzed the alternation of protein profile expression compared to the control group. Notably, the protein abundance at 49kDa, which is the molecular weight of c-MYC remarkably decreased after the deletion of eIF4A1 (additional file 1: Figure S1).

Gene Ontology (GO) analysis revealed that the DEPs enriched in the GO terms for 497 biological processes (BPs), 56 cellular components (CCs), 48 molecular functions (MFs) with statistical significance (Fig. 2b). Through the GO analysis, we can conclude that the DEPs enriched in metastasis relevant functions including signal transduction, cytoskeleton, lymph-angiogenesis, cell junction. Gene set enrichment analysis (GSEA) performed with ribosomal profiling showed that the enrichment of EMT-related gene sets reduced significantly after CR31B treatment (Fig. 2c). These results indicated that eIF4A1 could target c-MYC to regulate the biological behaviors of pancreatic cancer cells.

eIF4A1 promoted EMT and metastasis through c-MYC/miR-9 signaling

Recent studies have demonstrated that c-MYC promoted EMT through upregulating the expression of miR-9, and miR-9 could competitively bind with E-cadherin encoding sequence which led to EMT occurrence (20, 28). Before exploring the role of eIF4A1 and c-MYC in the regulation effect in pancreatic cells, we analyzed the expression of eIF4A1 in pancreatic cell lines Panc-1, Capan-2, AsPC-1, MiaPaca-2, and normal pancreatic ductal epithelial cell line HPDE. Western blot showed that eIF4A1 was notably higher expressed in the aggressive pancreatic cancer cell line AsPC-1 and relatively lower expressed in the indolent Capan-2 cell line and normal HPDE cell line (Fig. 3a). Therefore, we selected AsPC-1 and Capan-1 in the follow-up studies. We repressed the eIF4A1 or c-MYC expression in aggressive AsPC-1 cells (eIF4A1 siRNA, c-MYC siRNA) and overexpressed the eIF4A1 or c-MYC expression in indolent Capan-2 cells (pcDNA3.1-eIF4A1, pcDNA3.2-myc). Western blot and qRT-PCR showed that down-regulation of eIF4A1 in aggressive AsPC-1 decreased the expression of EMT-related gene (c-MYC, snail, and miR-9) and increased the expression of E-cadherin (Fig. 3b). Downregulation of c-MYC resulted in the same expression alternation (Figure, 3c), however, repressing the c-MYC expression did not influence the expression of eIF4A1. Accordingly, the results of eIF4A1 and c-MYC upregulation in Capan-2 were consistent with the trends of downregulation experiments (Fig. 3d, 3e). Transwell migration and invasion assays showed that eIF4A1/c-MYC-downregulated AsPC-1 cells displayed significantly lower migratory and invasive abilities (Fig. 3f), and the abilities of eIF4A1/c-MYC upregulated Capan-2 cells increased significantly than control (Fig. 3g). Based on the changes of EMT-related molecule expression level and the changes of migratory

and invasive capabilities, these results indicated that eIF4A1 could promote EMT through targeting c-MYC/miR-9 signaling.

Overexpression of eIF4A1 increased the MYC-downregulated AsPC-1 cells' invasive, migratory, and metastatic capabilities in vitro and in vivo

The relation between eIF4A1 and c-MYC is not simply direct upstream and downstream, recent studies revealed that overexpressed c-MYC could increase the expression level of eIF4A1 reversely (15, 29). To further explore the regulatory relations between eIF4A1 and c-MYC, lentivirus was used to regulate the eIFA1 and c-MYC expression. The setting groups were as follow: 1) e-U-M-D sequential regulation group: overexpressed eIF4A1 expression (Lv- eIF4A1) of AsPC-1 followed by repressing c-MYC expression (Lv-sh-c-MYC); 2) e-U group: singly overexpressed eIF4A1 (Lv- eIF4A1) expression; 3) M-D group: singly repressed c-MYC (Lv-sh-c-MYC) expression; 4): Vector group (Lv-sh-control).

Western blots showed that the expression level of E-cadherin significantly decreased in e-U AsPC-1 cells, and significantly increased in the M-D AsPC-1 cells. The E-cadherin expression level of e-U- M-D AsPC-1 cells was between e-U group and M-D group, however, still higher than the level of vector group cells (Fig. 4a). Consistent with the trends of western blot results, Transwell migration and invasion assays showed that the migratory and invasive abilities of e-U- M-D sequential regulation group cells were superior to the M-D group cells, but inferior to the vector group and e-U group (Fig. 4b). In vivo, the metastatic potentials of the above group cells were examined using a mouse metastasis model via caudal vein injection. The results (Fig. 4c) also showed that the luminescence intensity of e-U-M-D group cells was significantly higher than M-D group cells (1.008e + 10 vs 5.387e + 9, $P = 0.0349$), accordingly weaker to the e-U group cells (1.008e$_+$ 10 vs 2.410e$_+$ 10, $P = 0.2369$). Collectively, both in vitro and in vitro results showed that the EMT level and metastatic capabilities of e-U- M-D sequential group cells were between e-U group and M-D group. These results indicated that overexpression of eIF4A1 expression could attenuate the inhibition of MYC-downregulated pancreatic cancer cells' capabilities of EMT and metastasis.

RocA alone was not inferior to RocA plus Mycro3 joint intervention to inhibit EMT and metastasis in vitro and in vivo

Our previous studies demonstrated that c-MYC was not the only target of eIF4A1 to promote EMT and metastasis. When c-MYC was repressed, eIF4A1 might expert pro-EMT effect through other pathways to compensate for the inhibition. Considering the complex loop relation between eIF4A1 and c-MYC, we adopted joint intervention of RocA (eIF4A1 inhibitor) plus Mycro3 (c-MYC inhibitor) to explore whether joint intervention is superior to the two inhibitors intervention alone.

To select the optimal drug concentration, we conducted series of drug concentration gradient experiments. The western blot results showed that the expression level of eIF4A1 decreased significantly at 100nM RocA and the expression level of c-MYC decreased significantly at 5000nM Mycro3 (Fig. 5a). There was crystal precipitation when concentration increasing. Thus, we selected 100nM RocA and

5000nM Mycro3 in the follow-up studies. To compare the safety and efficiency of different intervention methods, we set 4 groups: 1) RocA + Mycro3 group; 2) RocA group; 3) Myro3 group; 4) DMSO control group. Western blots and qRT-PCR showed that all 3 intervention methods significantly increased the E-cadherin expression level and decreased the c-MYC expression level of AsPC-1 cells (Fig. 5b). Compared with the control group, all 3 intervention methods also remarkably decreased the migratory and invasive abilities. All 3 intervention methods could decrease the EMT level of pancreatic cancer cells (Fig. 5c). However, there was no statistical significance among the 3 groups.

To examine the efficiency and safety of different intervention methods in vivo, we used a mouse metastasis model via caudal vein injection. We found that the mouse mortality rates of RocA group (40.0%) and joint intervention group (62.5%) were relatively high. The autopsy showed that there were multiple cases present with nonocclusive intestine dilation. Considering the possible high-dose and frequent RocA use induced intolerance, we decreased the dose intensity from 5mg/kg/d qd to 2.5mg/kg/d once on alternate day by intraperitoneal injection, and the dosage of mycro3 remains intragastric 100mg/kg/d qd. The mice were well-tolerant to the modified regimen without more death cases. The luminescence intensity from RocA single-dose group was significantly weaker than the control group (1.393e + 9 vs 2.707e + 9, $P = 0.0474$). However, there were no statistical differences in luminescence intensity between the control group and the myro3 single-dose group/ joint intervention group (Fig. 5d). Taken together, these data demonstrated that the modified regimen of RocA single-dose presented an obvious anti-metastasis effect, even superior to mycro3 or joint-intervention.

To further testify the efficacy of RocA, we used a subcutaneous xenograft nude mice model. The 2-way ANOVA analysis indicated that the tumor volumes of RocA group were significantly smaller than those of the control group ($P < 0.0001$) (Figure. 5e) which indicated that RocA notably suppressed the growth of tumor. And western blot showed that RocA markedly decreased the expression of eIF4a1, c-MYC, and snail whereas increased the expression of E-cadherin (Fig. 5f) in vivo.

Discussion

Various PDAC involved oncogenes including KRAS and downstream kinases cannot be targeted because of their specific molecular structures (23, 30). However, targeting the translational procedure has been an alternative option for cancer treatment. The protein production of PDAC was verified to be hyperactive both *in vivo* and in organoids (31). And eIF4A which participates in the assembly of eIF4F, is the nexus for translational regulation (13, 32). Unlike KRAS, eIF4A could be targeted and the curative effects have been validated in several hematological malignancies (25, 33). Thus, targeting eIF4A could be an alternative treatment for PDAC.

Our previous study demonstrated targeting eIF4A could significantly decrease the lung metastasis of pancreatic cancer cells *in vivo* (26). Here we further represent the mechanism of eIF4A promoting EMT and metastasis and verified the overexpression of eIF4A1 was correlated with poorer prognosis. Considering the complex long-sequence 5'-UTR structure of c-MYC mRNA, we demonstrated that the

expression regulation of c-MYC was highly dependent on eIF4A. Depletion of eIF4A1 significantly decreased the expression level of c-MYC and pro-EMT molecules *in vitro*. Overexpression of eIF4A1 induced E-cadherin expression decreasing thorough c-MYC/miR-9 axis. Furthermore, depletion of eIF4A1 or c-MYC significantly decreased the EMT level and metastasis *in vitro* and *in vivo*, and vice versa. However, the regulation of translational regulation was extremely complicated. c-MYC cannot be the only target for eIF4A1 to promote EMT and metastasis and it was reported that c-MYC overexpression could reversely upregulate c-MYC (29, 34). In this study, we found that overexpression of eIF4A1 rescued the impaired EMT and metastasis capabilities of c-MYC repressed pancreatic cancer cells *in vitro* and *in vivo*. Nevertheless, the compensation for c-MYC depletion was not complete. The metastasis capabilities of e-U-M-D cells were significantly weaker than e-U cells whereas stronger than M-D cells. This result proved that even if there may exist other targets of eIF4A1, c-MYC still played a vital role in eIF4A-mediated EMT and metastasis.

Similar to KRAS, c-MYC was traditionally deemed as an “undruggable” target. Mycro3 was a novel anti-MYC compound to inhibit c-MYC activity through MYC-dimerization (23, 35). As previously mentioned, the relation between eIF4A and c-MYC was not simply unidirectional, thus, adopted eIF4A and c-MYC joint intervention to testify the efficacy and safety. Our works demonstrated single-use of RocA or Mycro3, and joint remedies all notably repressed the EMT level in *vitro*. However, the joint intervention did not show any superiority compared with single-use. Similar to the *in vitro* result, RocA was the only reagent that showed a significant anti-metastasis effect *in vivo* among two single-use remedies and joint intervention. The reason leading to this result is still unknown, but we can speculate from the preparatory experiments that joint intervention of RocA plus mycro3 increased the risk of death. The mice may not be tolerant of the original dose. But regardless, Roc single-use dramatically suppressed the eIF4A-mediated pancreatic cancer cell metastasis.

Conclusions

Collectively, we demonstrate that eIF4A1 overexpression downregulated E-cadherin expression through c-MYC/miR-9 axis, which promoted EMT and metastasis of pancreatic cancer cells *in vitro* and *in vivo*. The upregulation of eIF4A1 could partially rescue the c-MYC-depletion mediated inhibition of EMT and metastasis. Moreover, RocA single-use was superior to the joint remedies the at current dose possibly due to the intolerance. Our works indicated that eIF4A1 was a satisfying biomarker for PDAC prognosis, and intervention of eIF4A1 provide a promising therapeutic strategy for PDAC metastasis.

Abbreviations

PDAC	pancreatic ductal adenocarcinoma
eIF	eukaryotic translation initiation factor
EMT	epithelial mesenchymal-transition
RocA	Rocaglamide
TCGA	The Cancer Genome Atlas
GTEx	Genome Tissue Expression
5’-UTR	5’-untranslated region
FC	fold change
FDR	false discovery rate
DEP	differential expressed protein

Declarations

Ethics approval and consent to participate:

The study concerning the clients’ right to privacy. The study was approved by the Ethical Committee of Tongji Hospital, Tongji Medical College, Huazhong University of Science and Technology and was conducted according to the principles of the Declaration of Helsinki. Written informed consent was obtained from the subject, and his study considered declaration of Helsinki as a statement of ethical principles. Informed consent was obtained from all patients.

Consent for publication

N/A

Availability of data and material

The datasets used and/or analyzed during the current study available from the corresponding author on reasonable request.

Competing Interests:

Drs. Yuchong Zhao, Yun Wang, Wei Chen, Shuya Bai, Wang Peng, Mengli Zheng, Yilei Yang, Bin Cheng, and Zhou Luan have no conflicts of interest or financial ties to disclose.

Funding

This work is supported by the National Natural Science Foundation of China, granted number: No.81802427), and the Wuhan Science and Technology Bureau granted number:

No.20190207010114310.

Authors' contributions:

B.C. and L.Z. designed the study and performed data analysis. Y.Z. and Y.W. performed acquisition of data. Y.Z. drafted the manuscript. W.Y. provided critical revision of the manuscript for important intellectual content. W.C., S.B., W.P., M.Z. and Y.L. performed technical support. Y. D. provided pathological verification. B.C. and L.Z. performed study supervision. All authors have read and approved the manuscript.

Acknowledgments

We sincerely thank all staff from the Tongji Hospital, Tongji Medical College, HUST for their effort in project execution. We also thank the statistical staffs (Ping Yin, Chang Shu) at the Department of Epidemiology and Biostatistics, School of Public Health, Tongji Medical College, HUST and Hepatic Surgery Centre, Tongji Hospital, Tongji Medical College, HUST and support from Shou-jiang Tang, University of Mississippi Medical Center.

References

1. Sung H, Ferlay J, Siegel RL, Laversanne M, Soerjomataram I, Jemal A, et al. Global cancer statistics 2020: GLOBOCAN estimates of incidence and mortality worldwide for 36 cancers in 185 countries. Cancer J Clin. 2021;70(4):313.
2. Siegel RL, Miller KD, Fuchs HE, Jemal A. Cancer Statistics. 2021. CA: a cancer journal for clinicians. 2021;71(1):7–33.
3. Pereira SP, Oldfield L, Ney A, Hart PA, Keane MG, Pandol SJ, et al. Early detection of pancreatic cancer. The lancet Gastroenterology & hepatology; 2020.
4. Rhim AD, Mirek ET, Aiello NM, Maitra A, Bailey JM, McAllister F, et al. EMT and dissemination precede pancreatic tumor formation. Cell. 2012;148(1–2):349–61.
5. Magliano MPD, Logsdon CD. Roles for KRAS in Pancreatic Tumor Development and Progression. Gastroenterology. 2013;144(6):1220–9.
6. Hendifar AE, Blais EM, Ng C, Thach D, Gong J, Sohal D, et al. Comprehensive analysis of KRAS variants in patients (pts) with pancreatic cancer (PDAC): Clinical/molecular correlations and real-world outcomes across standard therapies. J Clin Oncol. 2020;38(15_suppl):4641.
7. Varga A, Soria JC, Hollebecque A, LoRusso P, Bendell J, Huang SMA, et al. A First-in-Human Phase I Study to Evaluate the ERK1/2 Inhibitor GDC-0994 in Patients with Advanced Solid Tumors. Clin Cancer Res. 2020;26(6):1229–36.
8. Van Cutsem E, Hidalgo M, Canon JL, Macarulla T, Bazin I, Poddubskaya E, et al. Phase I/II trial of pimasertib plus gemcitabine in patients with metastatic pancreatic cancer. Int J Cancer. 2018;143(8):2053–64.

9. Bedard PL, Tabernero J, Janku F, Wainberg ZA, Paz-Ares L, Vansteenkiste J, et al. A Phase Ib Dose-Escalation Study of the Oral Pan-PI3K Inhibitor Buparlisib (BKM120) in Combination with the Oral MEK1/2 Inhibitor Trametinib (GSK1120212) in Patients with Selected Advanced Solid Tumors. Clin Cancer Res. 2015;21(4):730–8.
10. Silvera D, Formenti SC, Schneider RJ. Translational control in cancer. Nature reviews Cancer. 2010;10(4):254–66.
11. Clemens MJ. Targets and mechanisms for the regulation of translation in malignant transformation. Oncogene. 2004;23(18):3180–8.
12. Raza F, Waldron JA, Le Quesne J. Translational dysregulation in cancer: eIF4A isoforms and sequence determinants of eIF4A dependence. Biochem Soc Trans. 2015;43(-):1227–33.
13. Boussemart L, Malka-Mahieu H, Girault I, Allard D, Hemmingsson O, Tomasic G, et al. eIF4F is a nexus of resistance to anti-BRAF and anti-MEK cancer therapies. Nature. 2014;513(7516):105–9.
14. Gingras AC, Raught B, Sonenberg N. eIF4 initiation factors: effectors of mRNA recruitment to ribosomes and regulators of translation. Annual review of biochemistry. 1999;68(-):913–63.
15. Wiegering A, Uthe FW, Jamieson T, Ruoss Y, Huettenrauch M, Kuespert M, et al. Targeting Translation Initiation Bypasses Signaling Crosstalk Mechanisms That Maintain High MYC Levels in Colorectal Cancer. Cancer discovery. 2015;5(7):768–81.
16. Spriggs KA, Cobbold LC, Jopling CL, Cooper RE, Wilson LA, Stoneley M, et al. Canonical initiation factor requirements of the Myc family of internal ribosome entry segments. Molecular cellular biology. 2009;29(6):1565–74.
17. Yourik P, Aitken CE, Zhou F, Gupta N, Hinnebusch AG, Lorsch JR. Yeast eIF4A enhances recruitment of mRNAs regardless of their structural complexity. Elife. 2017;6(-):e31476.
18. Sodir NM, Swigart LB, Karnezis AN, Hanahan D, Evan GI, Soucek L. Endogenous Myc maintains the tumor microenvironment. Genes Dev. 2011;25(9):907–16.
19. Ischenko I, Zhi J, Moll UM, Nemajerova A, Petrenko O. Direct reprogramming by oncogenic Ras and Myc. Proc Natl Acad Sci U S A. 2013;110(10):3937–42.
20. Ma L, Young J, Prabhala H, Pan E, Mestdagh P, Muth D, et al. miR-9, a MYC/MYCN-activated microRNA, regulates E-cadherin and cancer metastasis. Nat Cell Biol. 2010;12(3):247–56.
21. Khew-Goodall Y, Goodall GJ. Myc-modulated miR-9 makes more metastases. Nat Cell Biol. 2010;12(3):209–11.
22. Duffy MJ, O'Grady S, Tang M, Crown J. MYC as a target for cancer treatment. Cancer treatment reviews. 2021;94(-):102154.
23. Duffy MJ, Crown J. Drugging "undruggable" genes for cancer treatment: Are we making progress? Int J Cancer. 2021;148(1):8–17.
24. Iwasaki S, Floor SN, Ingolia NT. Rocaglates convert DEAD-box protein eIF4A into a sequence-selective translational repressor. Nature. 2016;534(7608):558–61.

25. Wu Y, Giaisi M, Kohler R, Chen WM, Krammer PH, Li-Weber M. Rocaglamide breaks TRAIL-resistance in human multiple myeloma and acute T-cell leukemia in vivo in a mouse xenogtraft model. Cancer Lett. 2017;389(-):70–7.
26. Luan Z, He Y, Alattar M, Chen ZS, He F. Targeting the prohibitin scaffold-CRAF kinase interaction in RAS-ERK-driven pancreatic ductal adenocarcinoma. Mol Cancer. 2014;13(-):11.
27. Wang X, Wang R, Bai S, Xiong S, Li Y, Liu M, et al. Musashi2 contributes to the maintenance of CD44v6 + liver cancer stem cells via notch1 signaling pathway. Journal of experimental clinical cancer research: CR. 2019;38(1):505.
28. Jackstadt R, Hermeking H. MicroRNAs as regulators and mediators of c-MYC function. Biochim Biophys Acta. 2015;1849(5):544–53.
29. Lin CJ, Cencic R, Mills JR, Robert F, Pelletier J. c-Myc and eIF4F are components of a feedforward loop that links transcription and translation. Cancer research. 2008;68(13):5326–34.
30. Dang CV, Reddy EP, Shokat KM, Soucek L. Drugging the 'undruggable' cancer targets. Nat Rev Cancer. 2017;17(8):502–8.
31. Boj SF, Hwang CI, Baker LA, Chio IIC, Engle DD, Corbo V, et al. Organoid Models of Human and Mouse Ductal Pancreatic Cancer. Cell. 2015;160(1–2):324–38.
32. Pelletier J, Graff J, Ruggero D, Sonenberg N. Targeting the eIF4F Translation Initiation Complex: A Critical Nexus for Cancer Development. Cancer research. 2015;75(2):250–63.
33. Yao C, Ni Z, Gong C, Zhu X, Wang L, Xu Z, et al. Rocaglamide enhances NK cell-mediated killing of non-small cell lung cancer cells by inhibiting autophagy. Autophagy. 2018;14(10):1831–44.
34. Castell A, Larsson L-G. Targeting MYC Translation in Colorectal Cancer. Cancer discovery. 2015;5(7):701–3.
35. Madden SK, de Araujo AD, Gerhardt M, Fairlie DP, Mason JM. Taking the Myc out of cancer: toward therapeutic strategies to directly inhibit c-Myc. Mol Cancer. 2021;20(1):3.

Figures

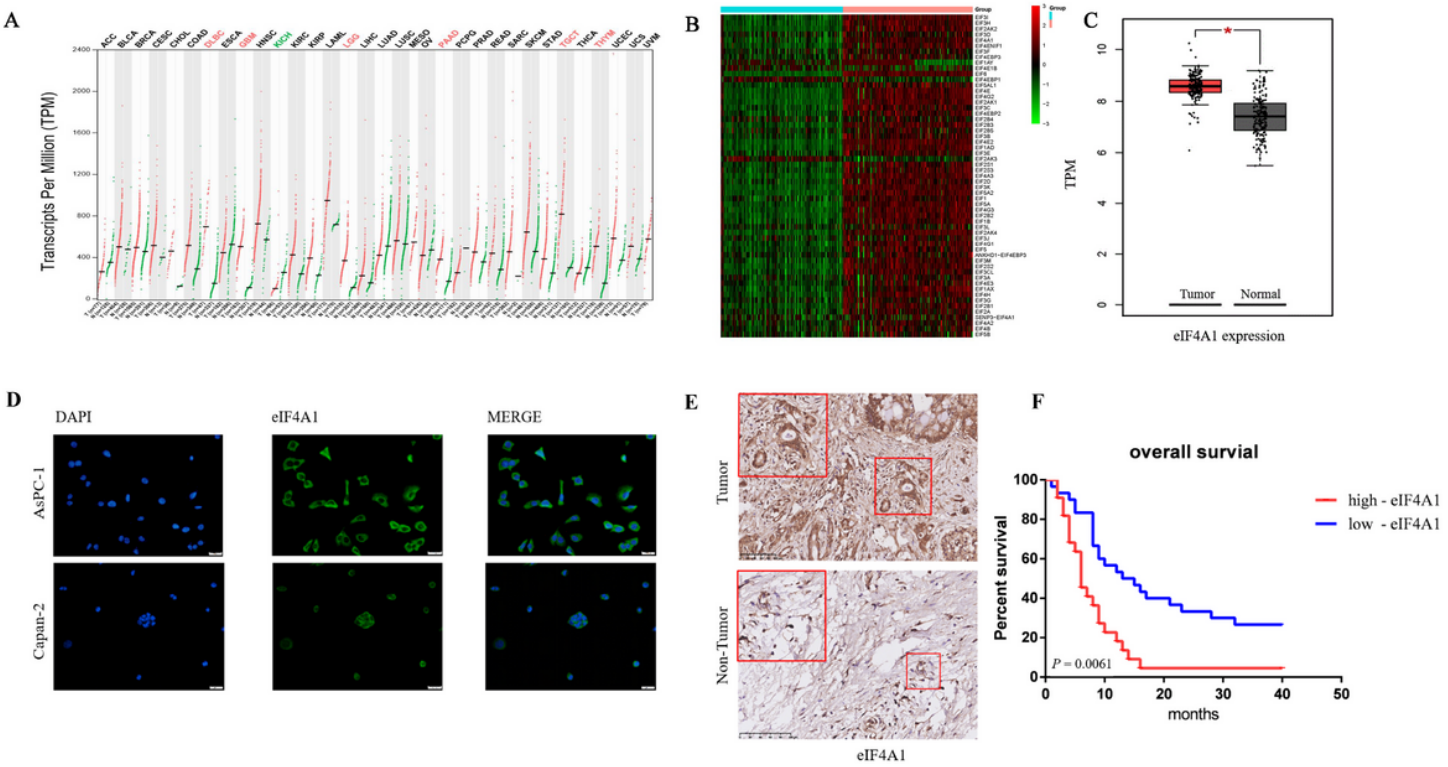

Figure 1

Analysis of the correlation of eIF4A1 expression and clinical features. (a). eIF4A1 was upregulated in various cancer types including pancreatic adenocarcinoma; (b) eIF4A1 was one of the top upregulated eIFs in PDAC; (c). eIF4A1 was significantly overexpressed in PDAC tumor tissues, log2[FC]= 1.162, P= 2.22e-16; (d). eIF4A1 was substantially located at cytoplasm; (e). Representative images of microarray IHC staining of MSI2 in tumor and adjacent non-tumor tissues, Scale bars: 100 μm; (f) survival analysis of overall survival were compared according to the expression levels of eIF4A1 in PDAC tissues. Patients with high eIF4A1 expression had shorter overall survival (6 months Vs. 9months, log-rank test, HR= 2.096, 95% CI: 1.438- 5.242, P= 0.0061).

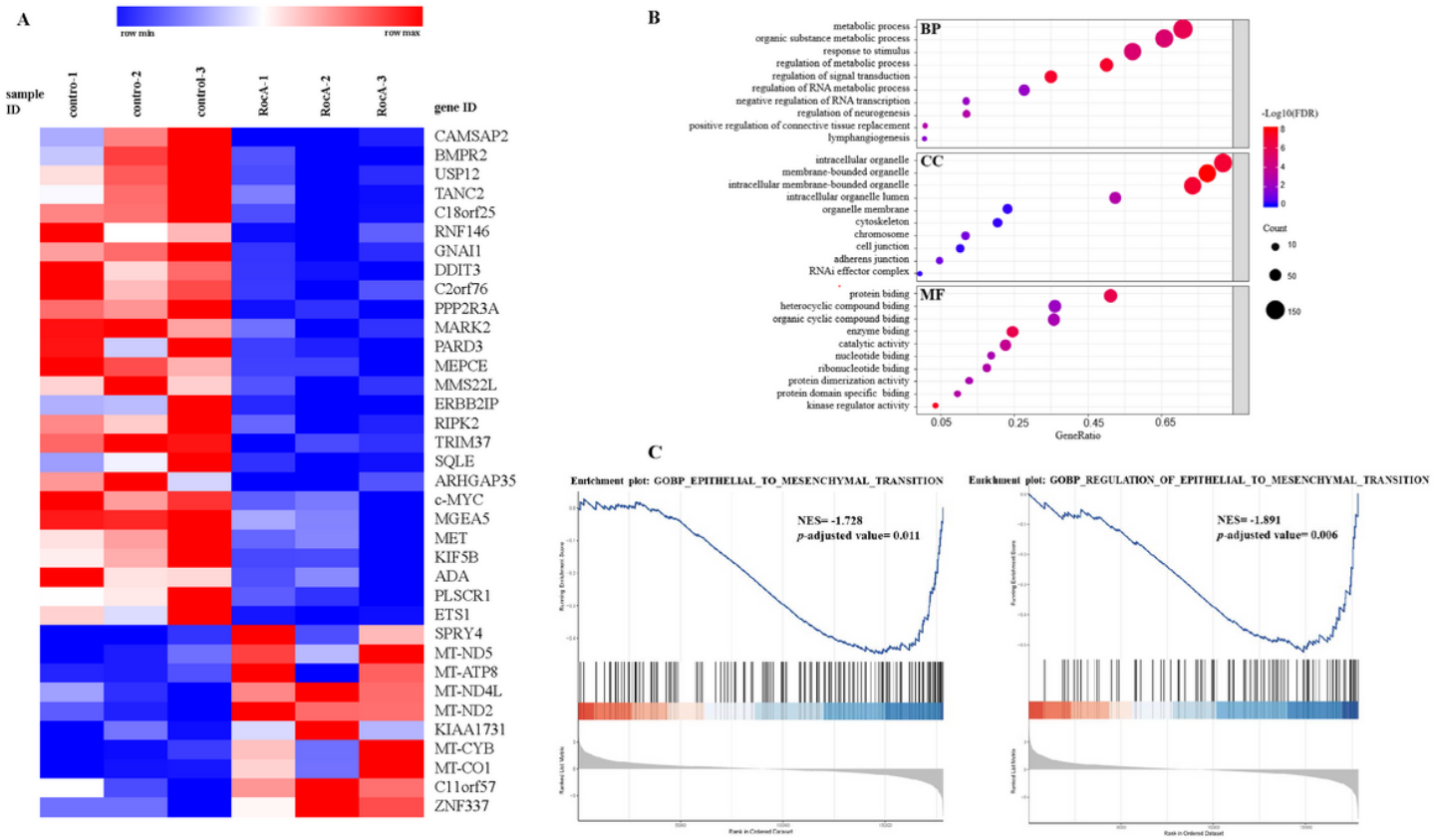

Figure 2

Screening the target of eIF4A1 in PDAC (a). The expression of c-MYC was significantly downregulated (log2FC = -1.05, FDR = 0.00192) in the CR31B-treated group compared with the control group, ranked the top 0.6% in all the regulated gene lists. (b). The differential expressed proteins were enriched in multiple metastatic-associated functions. (c). Gene set enrichment analysis was performed with ribosomal profiling results. Gene enrichment plots showed that the enrichment of EMT-related gene sets reduced substantially after eIF4A-intervention.

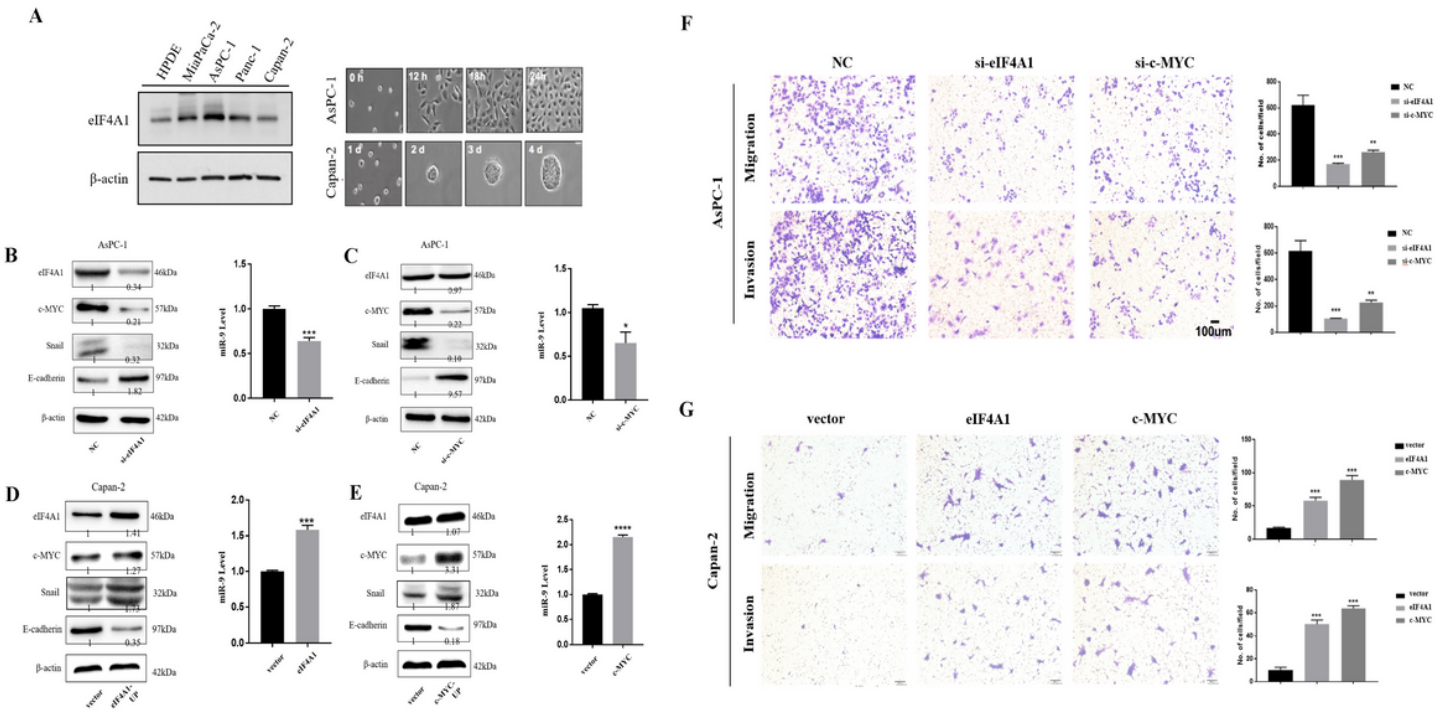

Figure 3

eIF4A1 targeted c-MYC to promote EMT in pancreatic cells (a). eIF4A1 was highly expressed in aggressive AsPC-1 cells and barely expressed in indolent Capan-2 cells. (b)-(c). downregulation of eIF4A1 or c-MYC increased the expression of E-cadherin whereas decreased the expression of snail and miR-9. Downregulation of eIF4A1 decreased the c-MYC expression, the expression changes of c-MYC did not influence the expression of eIF4A1. (d)-(e). Upregulation of eIF4A1 or c-MYC decreased the expression of E-cadherin whereas increased the expression of snail and miR-9. Upregulation of eIF4A1 increased the c-MYC expression, the expression changes of c-MYC did not influence the expression of eIF4A1. (f). Knockdown of eIF4A1 or c-MYC impaired the migratory and invasive capabilities of aggressive AsPC-1 cells. (g). Overexpression of eIF4A1 or c-MYC enhanced the migratory and invasive capabilities of indolent Capan-2 cells. *P< 0.05, **P<0.01, ***P< 0.001.

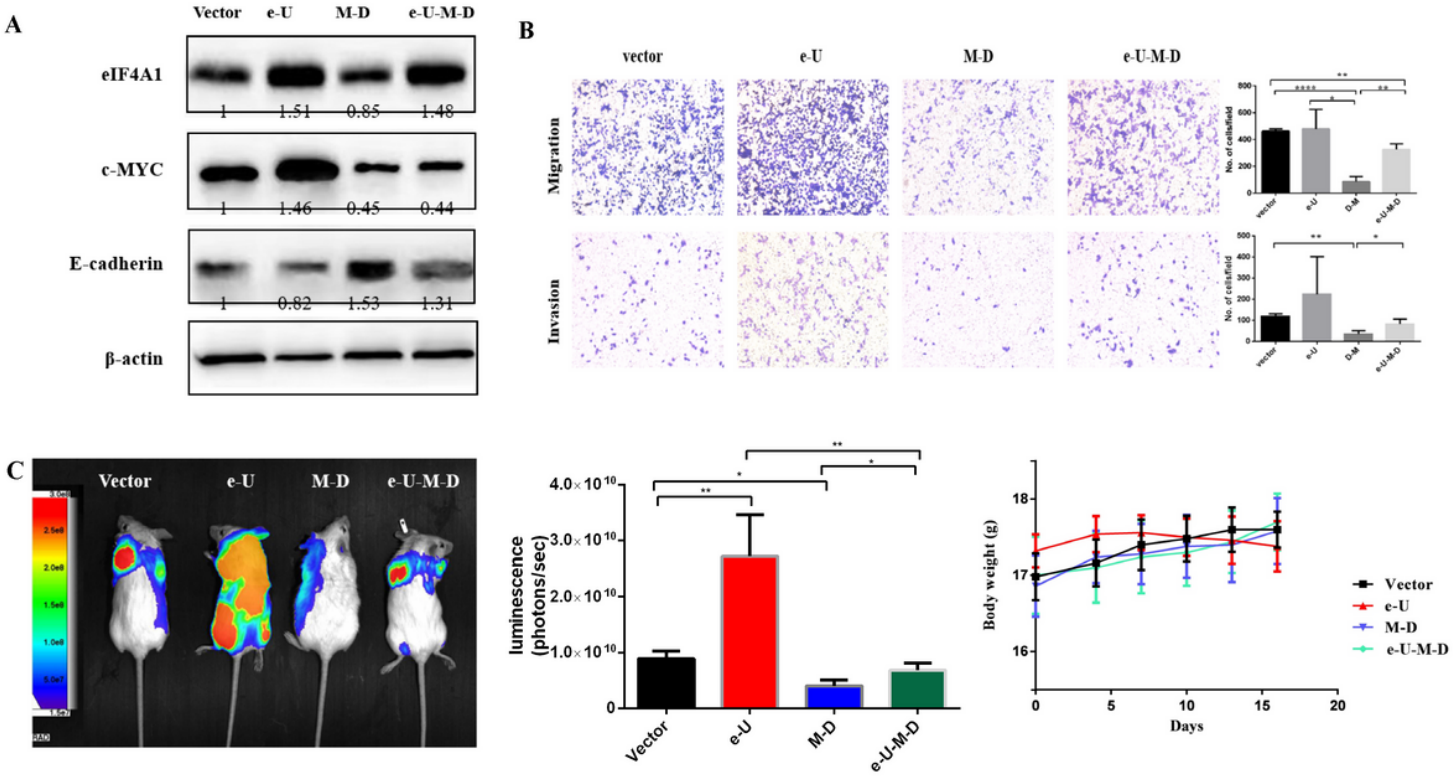

Figure 4

Sequential regulation of eIF4A1/c-MYC in vitro and in vivo. (a). the E-cadherin expression of e-U-M-D group AsPC-1 cells was between which of e-U group and M-D group AsPC-1 cells. (b) The migratory and invasive capabilities of e-U-M-D AsPC-1 cells were significantly stronger than M-D group cells. (c) The metastatic capabilities of e-U-M-D cells were between e-U and M-D group cells in vivo. *P< 0.05, **P<0.01, ***P< 0.001.

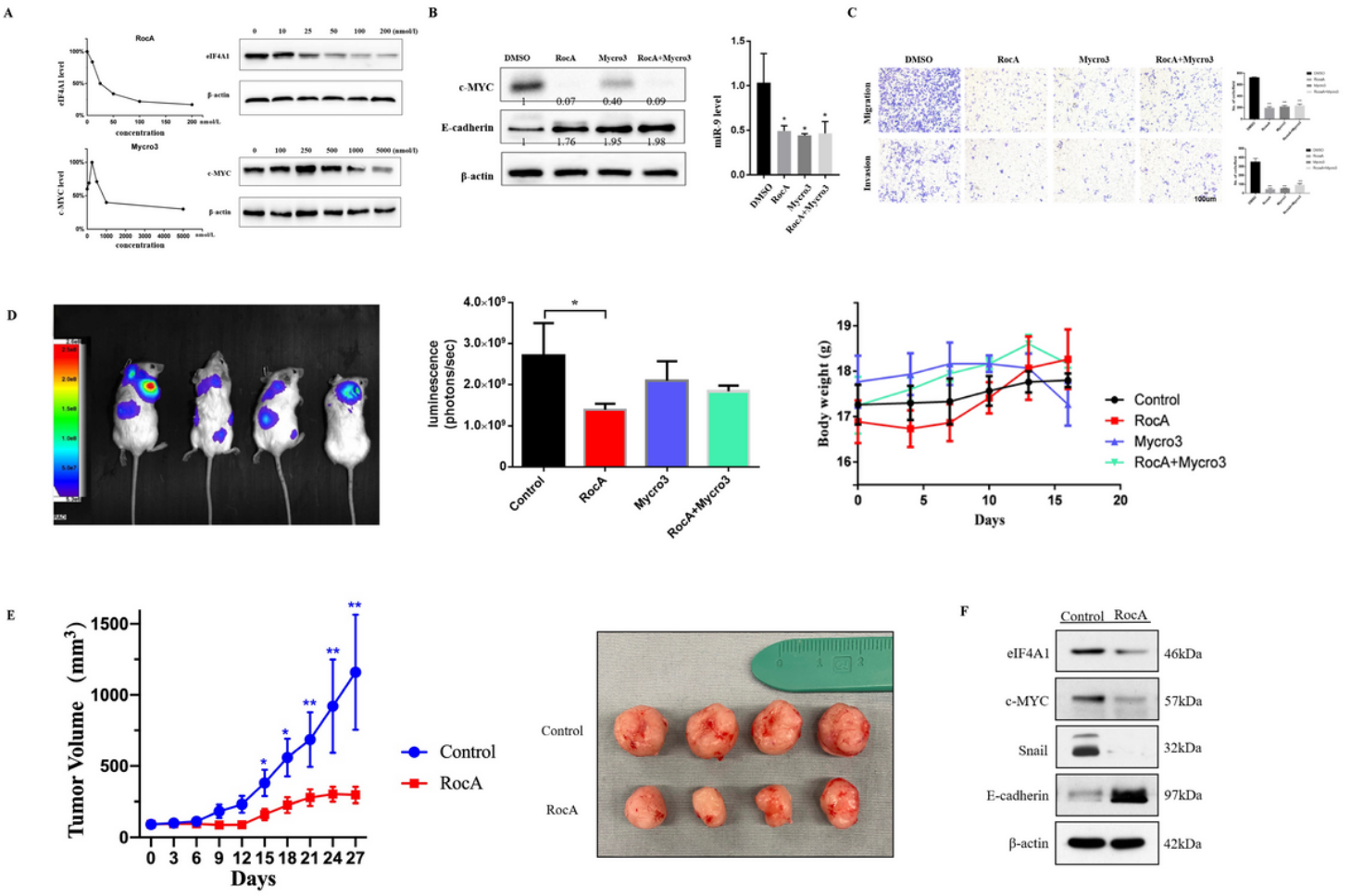

Figure 5

RocA and mycro3 suppressed pancreatic cancer cell EMT and metastasis in vitro and in vivo. (a). 100nmol/L (RocA) and 5000nmol/L (Mycro3) were the suitable intervention concentration. (b). 100nmol/L RocA, 5000nmol/L Mycro3, and joint intervention significantly inhibited the expression of miR-9 and c-MYC of AsPC-1 cells. (c) 100nmol/L RocA, 5000nmol/L Mycro3, and joint intervention significantly decreased the migratory and invasive capabilities of AsPC-1 cells. There were no statistical differences among each group. (d). RocA significantly decreased the metastasis level of AsPC-1 cells in vivo whereas mycro3 and joint intervention did not. (e) RocA significantly suppressed the subcutaneous tumor xenografts growth. (f) Western blot results showed that RocA notably decreased the eIF4A1, c-MYC, and snail expression, however, increased the E-cadherin expression in subcutaneous tumor grafts.

Supplementary Files

This is a list of supplementary files associated with this preprint. Click to download.

- FigureS1.tif